ACI STRUCTURAL JOURNAL TECHNICAL PAPER

Title No. 118-S96

Test of 90-Foot Post-Tensioned Concrete Girder with Unbonded Tendons

by Santiago Pujol, Damon R. Fick, and Luis B. Fargier-Gabaldón

A full-scale post-tensioned concrete girder with unbonded tendons was tested to investigate whether, under vertical forces, a full flexural mechanism (with three hinging regions) would form, and what strand stress would be reached in that condition. The specimen was a 0.91 m (3 ft) deep T-beam with a 2.43 m (8 ft) wide flange, spanning over two supports spaced at 18.3 m (60 ft) with two 4.6 m (15 ft) cantilevers and featured a parabolic tendon profile. Transverse reinforcement to resist shear and longitudinal "mild" reinforcement were also provided. A uniformly distributed load was applied on the main span and concentrated loads were applied to the ends of the cantilevers. While the main span was loaded, the two concentrated loads on the cantilevers provided a reaction force to minimize rotations at supports. At the end of the test, the girder deflected 278 mm (10.9 in., L/65) and carried 231 kN/m (15.5 kip/ft) over the main span. A full plastic mechanism formed with hinging regions at supports and at midspan. Test results suggest the unbonded tendons nearly reached their nominal strength (f_{pu}) and that a limit analysis is adequate for estimating the flexural strength of comparable post-tensioned girders.

Keywords: limit analysis; post-tensioned concrete; unbonded tendons.

INTRODUCTION

The flexural behavior of post-tensioned concrete flexural members with unbonded tendons under service conditions is well understood. Consensus exists in the profession that prior to cracking, increasing external moment demand is resisted by variations in the lever arm between the resultant compression force in the concrete and the nearly constant tension force in the tendons. It is also accepted that between cracking and ultimate loads, the stress in the unbonded tendon increases to match the external moment demand, while the distance between the force couple varies relatively little. The magnitude of this stress increase, however, is hard to estimate during the design process. A sectional analysis based on strain compatibility, as used for bonded tendons, is not applicable because in unbonded tendons, strains are averaged over their length, or a fraction of this length, which is hard to anticipate because of friction between the tendon and the ducts.

Several experimental research programs have been conducted to investigate the behavior of posttensioned beams with unbonded tendons at their ultimate moment strength in simple spans, including the works of Pannell (1969), Mattock et al. (1971), Tam and Pannell (1976), Cooke et al. (1981), Du and Tao (1985), Campbell and Chouinard (1991), Harajli and Kanj (1992), Chakrabarti (1995), Tan and Ng (1997), and Ng (2003). Specimens tested in these research programs featured simple spans ranging from 3 to 10 m. The testing of continuous spans imposes additional challenges as reported in the experimental research done by Burns and Hemakom (1977), Burns et al. (1978, 1991), Kosut et al. (1985), Hemakom (1970), Gebre-Michael (1970), Mattock et al. (1971), Chen (1971), Aravinthan et al. (1996, 2005), Harajli et al. (2002), Aparicio et al. (2002), Tan and Tjandra (2007), Decheng (2009), Lou et al. (2013), Zhou and Zheng (2014), and Maguire et al. (2015). In these experimental programs, continuous spans up to 6 m (20 ft) were tested.

Results from these experimental programs suggest that factors affecting the stress in the unbonded tendons at ultimate loads include, depth and length of the girder, depth of the neutral axis, amount of mild reinforcement, number of hinges leading to a collapse mechanism, Young's modulus of the tendon, among others. A summary of the most relevant aspects of these research programs can be found in Maguire et al. (2017).

This investigation focused on (a) the ability of a full-scale continuous post-tensioned girder with unboned tendons to develop a mechanism formed by plastic hinges over the supports and at midspan; and (b) the stress reached in the unbonded tendons at peak load.

RESEARCH SIGNIFICANCE

There is limited information from tests, under controlled laboratory conditions, for full-scale continuous beams with unbonded prestressing tendons. The available experimental information from small beams is useful but it is not easy to project because friction between strands and ducts/sleeves cannot be resolved through similitude without uncertainty. Information gathered from the testing of this 27.4 m (90 ft) long post-tensioned T-beam will help reduce uncertainty and provide information related to the stress of the unbonded tendon at ultimate loading for comparable beams.

EXPERIMENTAL INVESTIGATION

As part of this investigation, a 27 m (90 ft) full-scale post-tensioned girder with unbonded tendons was constructed, instrumented, and tested to failure in Bowen Laboratory at Purdue University, West Lafayette, IN, and is shown in Fig. 1.

ACI Structural Journal, V. 118, No. 5, September 2021.
MS No. S-2020-158, doi: 10.14359/51732860, received April 19, 2020, and reviewed under Institute publication policies.

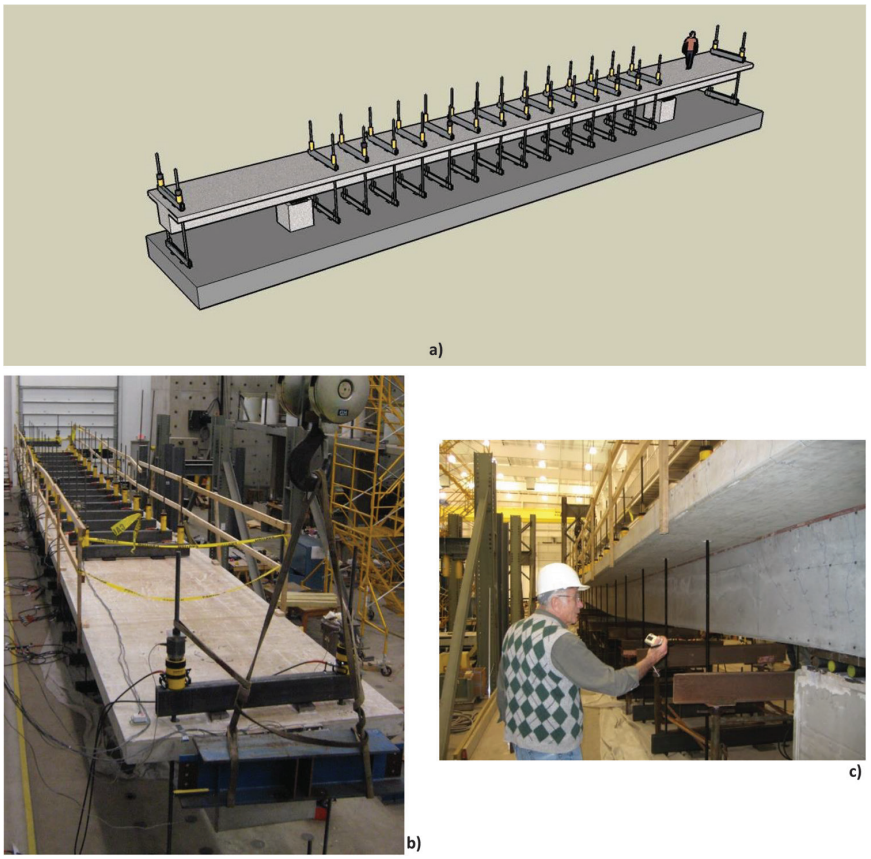

Fig. 1—(a) Test specimen, three-dimensional view; (b) test specimen view from above; and (c) side view of test specimen during loading and late Prof. Mete Sozen examining crack pattern.

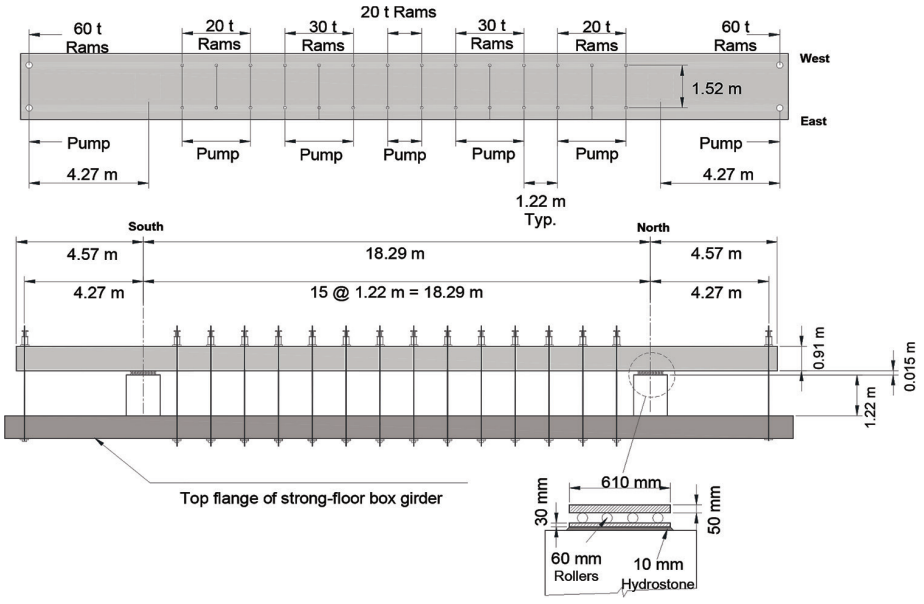

Fig. 2—Test specimen.

Specimen description

The 27.4 m (90 ft) long post-tensioned T-beam with a 2.43 m (8 ft) flange and depth of 0.91 m (3 ft) had a central span of 18.3 m (60 ft) with cantilevers extending 4.6 m (15 ft) at either end (Fig. 2). An approximately uniformly distributed load was applied over the central span using 28 hydraulic rams connected to threaded rods attached to the strong floor. A pair of concentrated forces was applied at the ends of each cantilever, to minimize rotation over the supports to obtain fixed-fixed support conditions. A plan and elevation view of the specimen is shown in Fig. 2.

The cross-sectional dimensions of the beam are shown in Fig. 3 and mild reinforcement in Fig. 4. After cracking and under positive bending moment at midspan, the 2.43 m (8 ft)

wide top flange, with a thickness of 0.23 m (7.5 in.), is in compression. Mild tension reinforcement at midspan was provided with eight 25 mm (No. 8) bars (resulting in a reinforcement ratio of 0.2%). Tension reinforcement over the south support consisted of twelve 25 mm bars (0.73% reinforcement ratio). The north support featured fifteen 25 mm (No. 8 bars) as tension reinforcement (0.91% reinforcement ratio). The different moment reinforcement ratios for negative bending over the supports reflected different adjacent span conditions of a prototype structure. The top flange of the girder was reinforced in the transverse direction with No. 4 bars (13 mm) at 0.30 m (12 in.).

Within the center span, closed stirrups around the outside perimeter of the girder were used, in combination with two single-leg ties (Fig. 5), while transverse reinforcement in the cantilevers consisted of two overlapping closed stirrups. In both cases, reinforcement consisted of four legs of 13 mm (No. 4 bars). Spacing of transverse reinforcement is shown in Fig. 6. Near midspan, transverse reinforcement was spaced at 0.61 m (24 in.; 0.67h) and near the supports, the spacing was reduced to 0.20 m (8 in.; h/4.5).

The beam was post-tensioned with 15 strands, 13 mm (1/2 in.) in diameter, distributed in three bundles, each with five strands. The average (mean) tendon profiles measured during the construction of the beam are shown in Fig. 7. Along the center span, the three bundles follow the same profile. Over the cantilevers, however, one bundle was placed with a uniform profile at approximately 0.81 m (32 in.) from the bottom of the girder, and the other two bundles were anchored at the cantilevered end at approximately 0.43 m (17 in.) from the bottom of the girder.

Load cells measured the force in five strands of the bundle that remained at 0.81 m (32 in.) above the bottom of the girder in the cantilever. Tendons were stressed from one end of the beam 22 days after concrete was cast. Average readings from these load-cells after losses from anchorage set was 1725 kN (380 kip; 0.64f_{pu}), while the measured elongation during stressing ranged from 170 to 190 mm (6-1/2 to 7-1/2 in.). The beam was tested 15 days after the tendons were stressed.

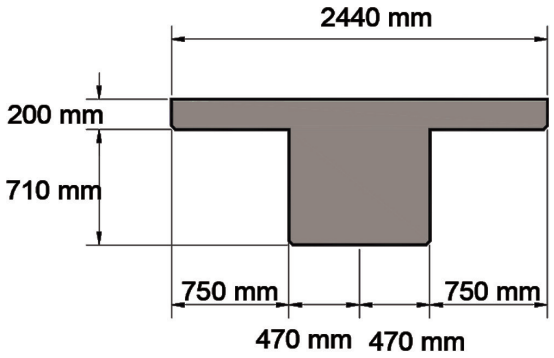

Fig. 3—Cross-sectional dimensions.

Material properties

Normal-weight aggregate air-entrained concrete was used. Mixture proportions per cubic yard are shown in Table 1. Portland cement type I (general use) was used because it is the most common type of cement used in the industry in applications where specific properties or exposures are not an issue. A total of 72 152 x 305 mm (6 x 12 in.) test cylinders were cast and cured under wet burlap for 7 days. At the time of maximum load application, cylinder tests indicated a mean compressive strength of 41 MPa (6 ksi). Grade 420 MPa (60 ksi) reinforcement was used for the mild longitudinal and transverse reinforcement. Three samples of the 25 mm (No. 8) bars used for

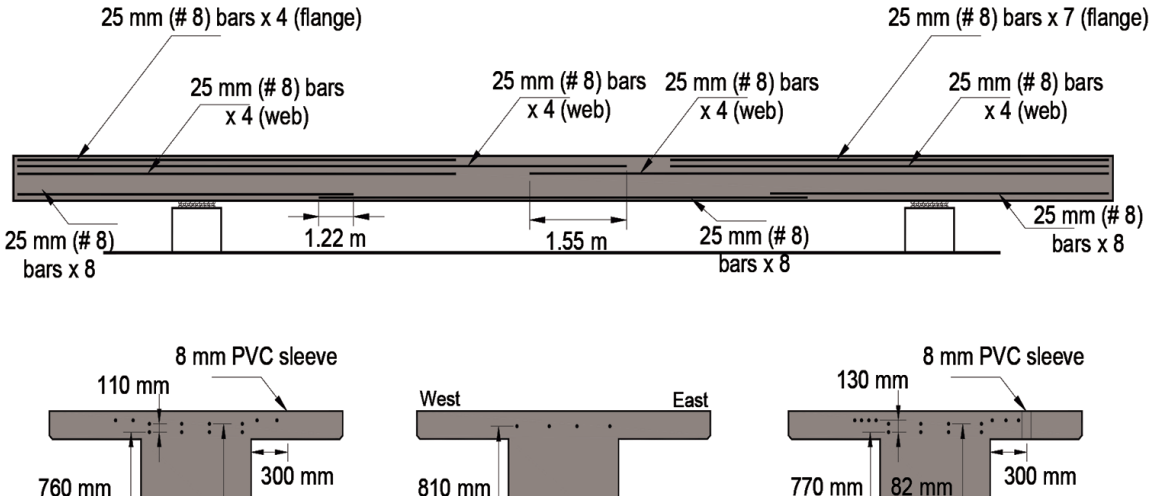

Fig. 4—Bonded reinforcement arrangement.

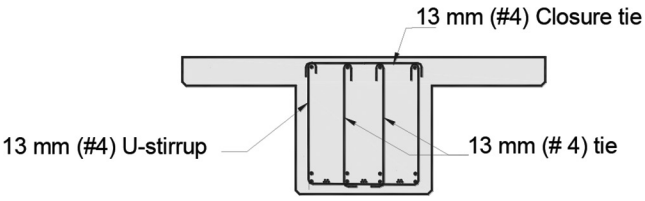

Fig. 5—Transverse reinforcement at midspan.

Table 1—Concrete mixture proportions (1 cubic yard)

w/c ratio	0.40
Sand	5595 N (1260 lb)
Aggregate (max. size: 3/4 in.)	8214 N (1850 lb)
Water	1075 N (242 lb)
Mid-range water reducer	24 oz per 444 N (100 lb) of cement

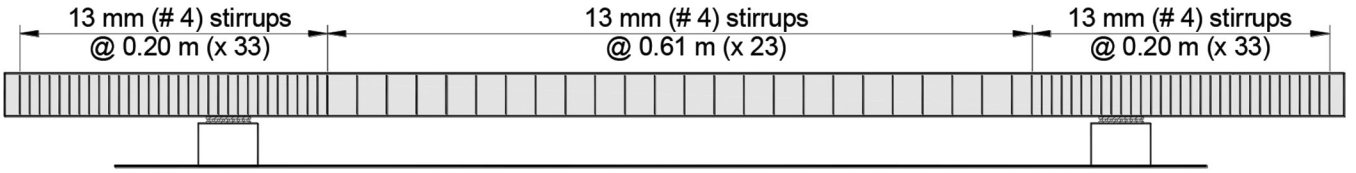

Fig. 6—Spacing of transverse reinforcement.

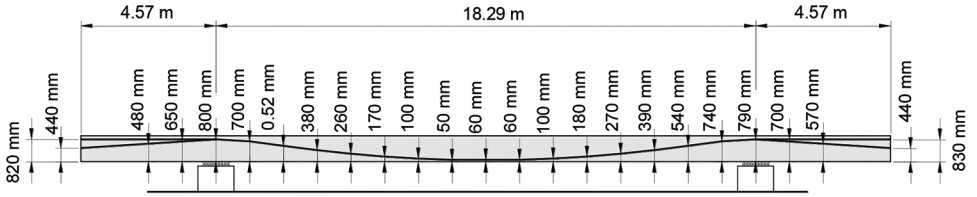

Fig. 7—Mean of measured values for three tendon profiles.

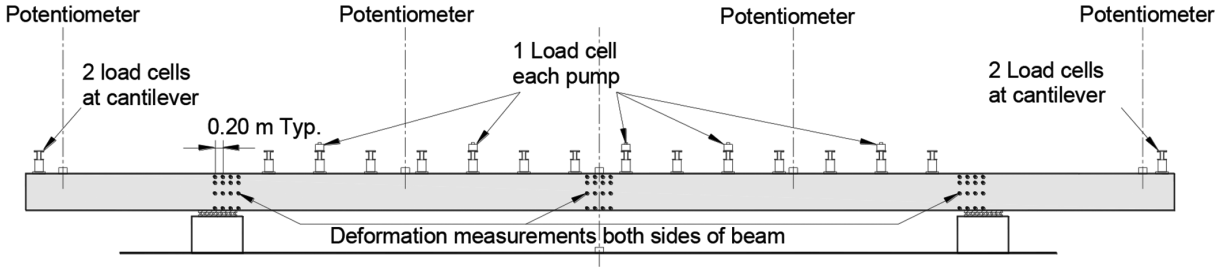

Fig. 8—Instrumentation.

the longitudinal reinforcement and three samples of the 13 mm (No. 4) bars used as transverse reinforcement were tested in tension. The measured mean yield stress was 441 MPa (64 ksi) for the 25 mm (No. 8) bars, while the mean strength was 703 MPa (102 ksi). The 13 mm (No. 4) reinforcing bars had a mean yield stress of 503 MPa (73 ksi) and a mean strength of 744 MPa (108 ksi). Low-relaxation steel, consisting of seven-wire strands with a nominal strength of 1860 MPa (270 ksi), were used as post-tensioned reinforcement.

Test setup

The test girder rested on two 0.91 m (3 ft) square piers spaced 18.3 m (60 ft) apart, with a height of 1.52 m (5 ft), that were cast on the strong floor of Bowen Laboratory. On top of each pier, a 25 mm (1 in.) thick steel plate was placed on a 13 mm (1/2 in.) layer of hydrostone to support four rollers with a diameter of 64 mm (2.5 in.) spaced at 150 mm (6 in.) in the direction of the girder span, as shown in Fig. 2. A steel plate, 610 x 910 x 5 mm (24 x 36 x 2 in.) with its 610 mm (24 in.) dimension parallel to the beam axis, rested on the rollers and supported the test girder (Fig. 2).

Instrumentation

Deflections were measured using potentiometers at five stations along the test girder, as shown in Fig. 8, while longitudinal deformations were measured over the supports and at midspan, using an electronic Whittemore gauge with a gauge length of 200 mm (8 in.). Rotations were measured over the centerline of the supports with inclinometers (approximately 50 mm [2 in.] long) installed 230 mm (9 in.) above the bottom face of the girder.

Loading protocol

The load on the main span was applied by sixteen 20-ton and twelve 30-ton hydraulic rams placed in pairs at intervals of 1.2 m (4 ft), as shown in Fig. 1, 2, and 8. While the main span was loaded, concentrated loads were applied on the cantilevers at 4.3 m (14 ft) from the center of each support, using pairs of 60-ton hydraulic rams. Details of the loading harnesses are shown in Fig. 9. Hydraulic pressure was applied to the rams within the central span using five pumps that were manually operated. Each pump controlled two or three loading harnesses (Fig. 9) as shown in Fig. 8. Loads were measured with load cells and monitored with calibrated pressure gauges connected to the pumps.

The test was conducted under a load-control protocol in three stages including loading, unloading, and reloading to failure. In the first loading stage, the applied load was increased up to 2110 kN (total load applied along the main span, including self-weight) and maintained for 24 hours prior to unloading. Then, in the unloading stage, the applied load was removed, and the beam supported its self-weight for 20 hours. Finally, the beam was reloaded to failure, which occurred at 4090 kN as explained next.

BEHAVIOR OF TEST SPECIMEN

The load versus deflection plot is shown in Fig. 10. First flexural cracking was observed at the north support, at a midspan deflection of 6 mm (0.24 in.) under a total applied load of 1400 kN including self-weight (310 kip), which corresponds to a uniformly distributed load of 79.2 kN/m (5.34 kip/ft). At this stage, crack widths did not exceed 0.05 mm (0.002 in.). As the load applied to the central span reached 1650 kN, 93.22 kN/m (365 kip, 6.29 kip/ft), a deflection of

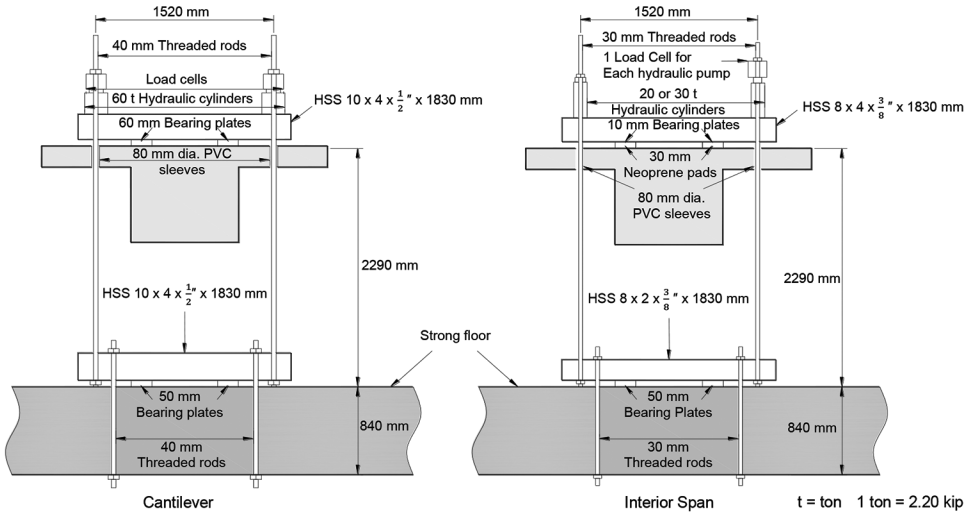

Fig. 9—Loading harness.

8.9 mm (0.37 in.) was observed, and new cracks were noticed. The maximum crack widths measured at this stage were 0.25, 0.20, and 0.50 mm (0.01, 0.008, and 0.02 in.) at north support, midspan, and south support, respectively. At 2110 kN (465 kip) of total load applied along the main span, which corresponds to 119 kN/m (7.93 kip/ft), the beam exhibited a midspan deflection of 23 mm (0.91 in.) and maximum crack widths measured were 0.8 mm (0.03 in.) at north support, 0.25 mm (0.01 in.) at midspan, and 0.90 mm (0.035 in.) at south support. The 2110 kN (119 kN/m) load was maintained for 24 hours and at the end of the 24-hour period, the midspan deflection had increased to 27 mm (1.06 in.). Then, the applied load was removed, leaving only the self-weight acting upon the girder (over the main span—this condition corresponds to a total applied load equal to 500 kN [110 kip], or 28.3 kN/m [1.8 kip/ft]), which resulted in a midspan deflection of approximately 4 mm (0.15 in.). After 20 hours under self-weight alone, the measured midspan deflection had not changed. Subsequently, the beam was then reloaded to failure. At a total load of 2656 kN (585 kip) over the main span, equivalent to 150 kN/m (10.1 kip/ft), the measured midspan deflection was 46 mm (1.8 in.) and maximum measured crack widths were 1 mm (0.04 in.) at the north support, 0.5 mm (0.02 in.) at midspan, and 1.3 mm (0.05 in.) at the south support.

Load increments were further applied to reach a midspan deflection of approximately 200 mm (8 in.) with the beam carrying a total load over the main span equal to 3930 kN or 222 kN/m (865 kip or 14.9 kip/ft). At this stage, loading was stopped and maintained for 24 hours and then resumed to reach 4090 kN or 231 kN/m (900 kip or 15.5 kip/ft) while the measured deflection was 276 mm (10.9 in.), that is $L/65$, approximately. At 4090 kN, one of the wedges that anchored a strand at the south end of the girder was ejected off its seat as a result of strand fracture somewhere along the beam. A segment of the fractured strand extended out of the concrete. At this point, the test was stopped. Another anchorage grip broke while the applied load was being reduced. Upon removing the applied load, the measured midspan deflection was 140 mm (5.4 in.).

Strains estimated from the measurements of longitudinal deformations described earlier are shown in Fig. 11. It is observed that strains exceeded 0.05 over a gauge length of

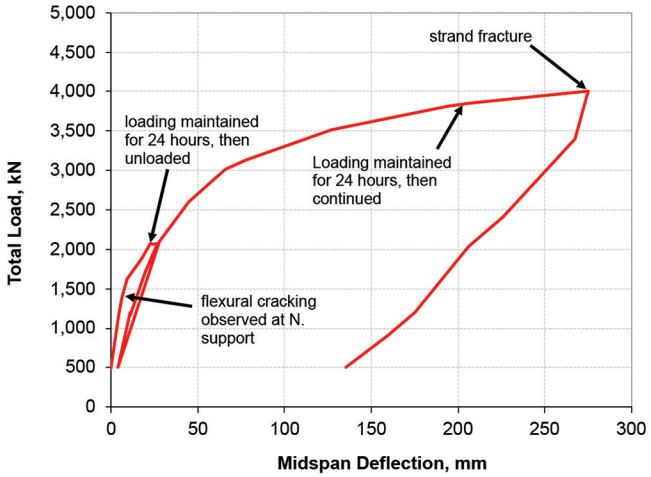

Fig. 10—Load-displacement response.

600 mm (24 in.) obtained through three measurements made with the 200 mm (8 in.) long gauge mentioned before. Crack patterns and a picture of the beam after the test was completed are shown in Fig. 12. Forces measured in the strands and forces applied to the cantilever free ends during the final loading to failure are shown in Fig. 13 and 14, respectively. The mean strand stress (measured in four out of 15 strands at the north end of the beam) was approximately 1200 MPa (175 ksi), while during the final loading to failure, the mean stress reached approximately 1600 MPa (235 ksi), with at least one instrumented strand reaching nearly 2000 MPa (290 ksi). It should be noted that load measurements from one of the four load cells applied to the cantilever free ends stopped recording at a load of 355 kN (80 kip).

Discussion

Estimated peak stresses in unbonded tendons at ultimate (f_{ps}) and the nominal moment capacity based on measured material properties are summarized in Table 2. In these equations, ρ_p is the prestressing reinforcement ratio; f_{pe} and f_{se} are the effective stresses in the tendon after losses (assumed as $0.60 \cdot f_{pu} = 1200$ MPa [175 ksi]); c is the depth of the neutral axis; and l_e is defined as $2 \cdot l_i/2 + N_s$, where l_i and N_s are the

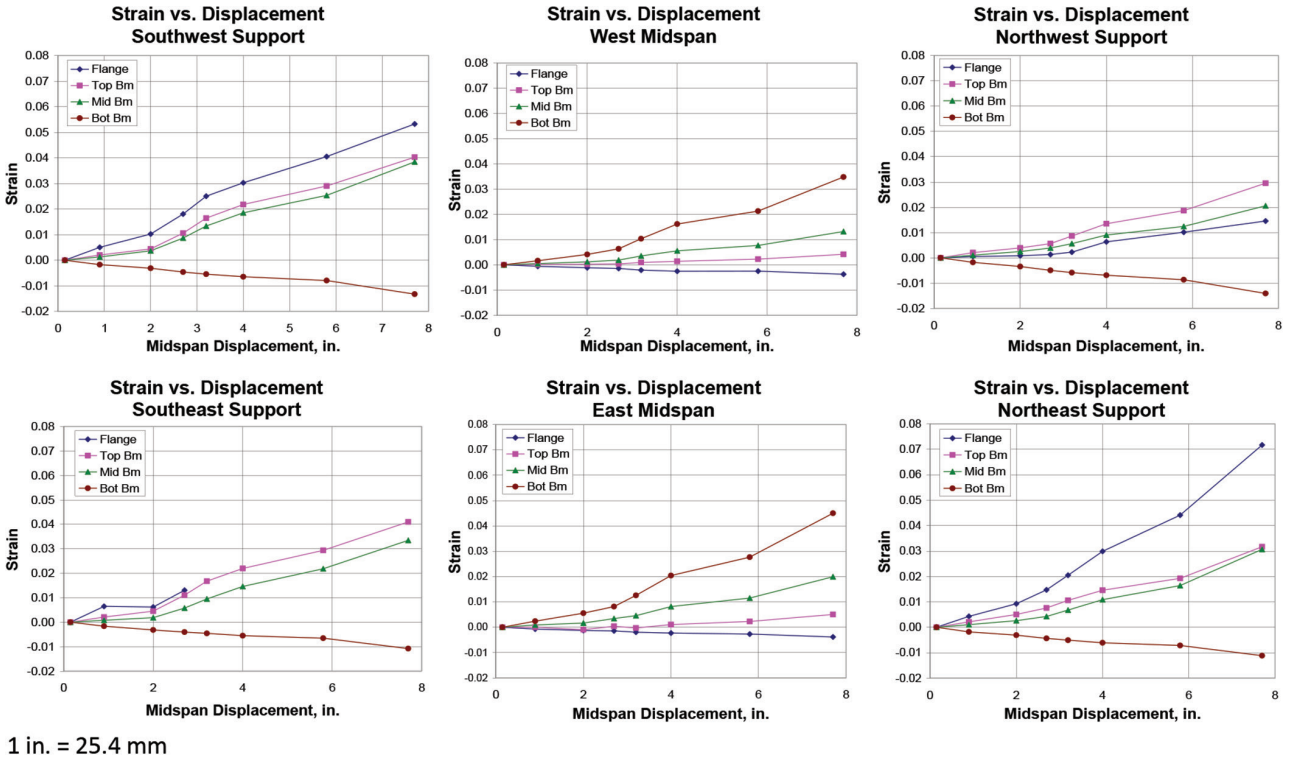

Fig. 11—Longitudinal concrete strain measurements.

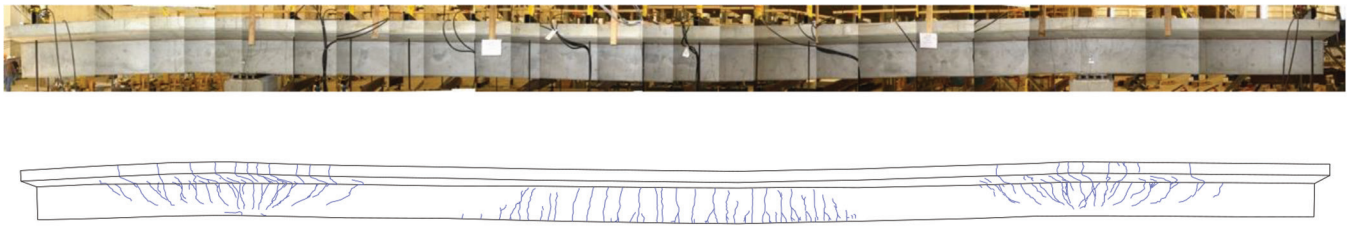

Fig. 12—East face elevation photo and cracking pattern map measurements.

length of the tendon between anchorages and the number of plastic hinges at supports, crossed by the tendon.

The test observations suggest full moment capacities were reached at supports and midspan. From a limit analysis, the load w leading to a mechanism is approximately

$$w = 8 \cdot \frac{\frac{M_l + M_r}{2} + M_c}{L^2}$$

where w is total uniform load in span L; M_l is moment capacity at left support; M_c is moment capacity at midspan; M_r is moment capacity at right support; and L is clear span.

For the ideal loading conditions, the previous expression is exact if the resisting moments at the supports are equal and provides satisfactory estimates of the load resistance even if one of the end moments is as low as 80% of the other end moment. It can also be modified easily to provide more reliable values if the end moments are more than 20% different from one another. For a 17.7 m (58 ft) clear span and the calculated nominal bending strengths shown in Table 2, a peak load $w \cong 190$ kN/m (≅12.5 kip/ft) is obtained for both the ACI 318-19 and AASHTO LRFD specifications (ACI Committee 318 2019; AASHTO 2018). The test beam, however, carried 4090 kN or 231 kN/m (900 kip or 15.5 kip/ft) over the central span. The actual strength of the test girder vis-à-vis its nominal strength is easily rationalized by noting that the strands were near their breaking loads when the peak load was reached. If the mean stress in the unboned tendons at peak load is taken as 1800 MPa (260 ksi; ~95% of its nominal strength) and the stress in the bonded reinforcement is taken as 560 MPa (80 ksi; ~ 80% of its strength), moment capacities shown in Table 2 increase approximately by 25% over the nominal values to approximately 4010 kN-m (2950 kip-ft) at midspan, 4350 kN-m (3200 kip-ft) over the south supports and 5300 kN-m (3900 kip-ft) over the north support, leading to w = 226 kN/m (15.5 kip/ft), that is 99% the peak load measured during testing, which suggests that the maximum applied load is consistent with the estimated plausible strengths of the three critical sections.

The increases in moment capacity, relative to nominal values, are consistent with (a) peak forces applied at the cantilevers (Fig. 14); and (b) strand stresses plotted in Fig. 13. Claim (a) requires the inclusion of self-weight and calculations of moments about the inner rollers at each support. (As strands became nonlinear, control of rotations over supports became more difficult. Given the stiffness of supports, even an infinitesimal rotation suffices to shift the reaction to the inner rollers.)

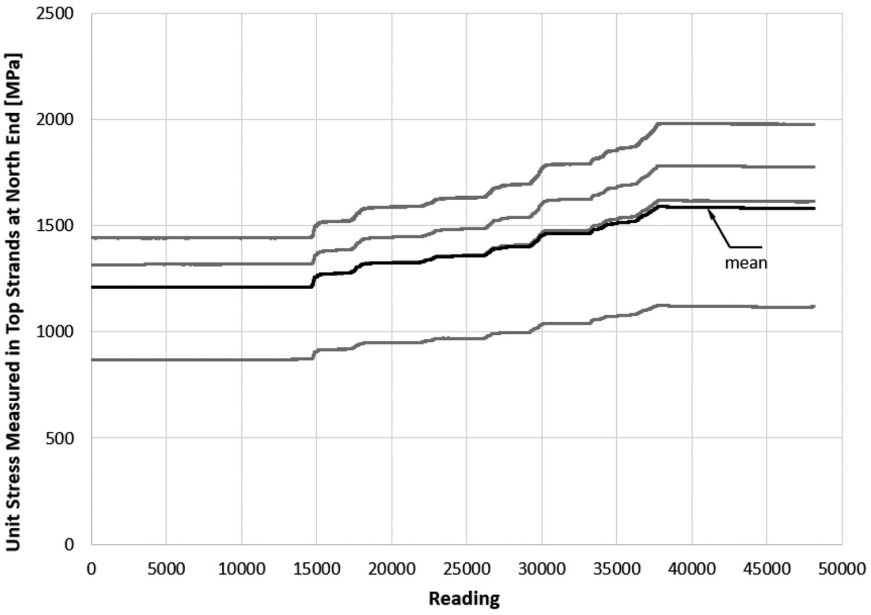

Fig. 13—Load cell readings (1.0 Hz) in final loading versus increase in strand stress.

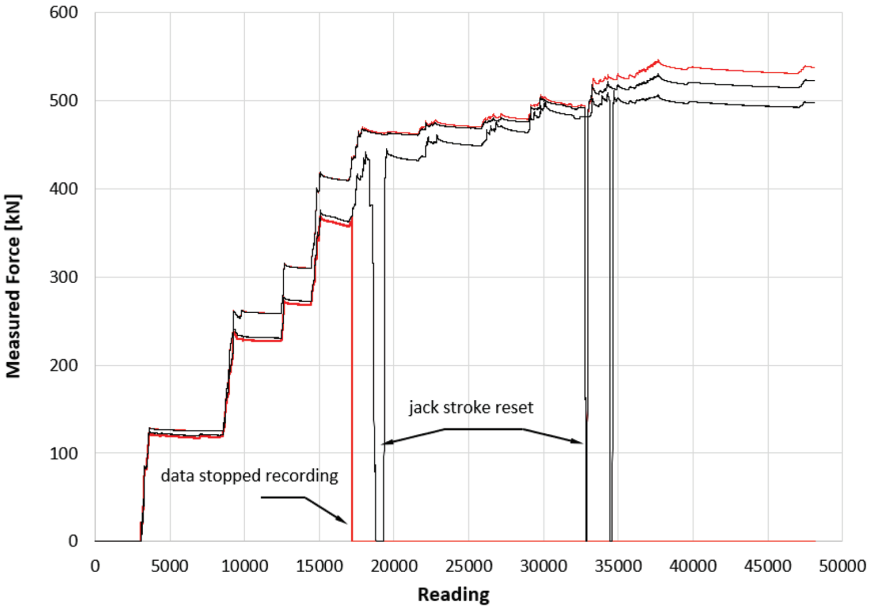

Fig. 14—Load cell readings (1.0 Hz) versus forces applied on overhangs.

Table 2—Calculated stress in unbonded tendon and nominal moment strength

Code	Equation/quantity	North and south support f_{ps}/f_{pu} M_n, N-m (kip-ft)	Midspan f_{ps}/f_{pu} M_n, N-m (kip-ft)
ACI 318-19 (20.3.2.4)	(a) $f_{ps} = f_{se} + 10 + \frac{f'_c/1000}{100 \cdot \rho_p}$	$f_{ps}/f_{pu} = 0.75$	$f_{ps}/f_{pu} = 0.91$
	(b) $f_{ps} = f_{se} + 60$	0.82	0.77
	(c) $f_{ps} = f_{py}$	0.90	0.90
	Min (a, b, c)	0.75	0.77
	Nominal moment capacity (M_n)	South: 3600 kN.m (2650 kip.ft) North: 4050 kN.m (2980 kip.ft)	3400 N.m (2500 kip.ft)
AAASHTO LRFD 2018 (5.6.3.1.2)	(d) $f_{ps} = f_{pe} + 900 \cdot \frac{(d_p - c)}{l_e}$	0.75 South: 3550 kN.m (2620 kip.ft) North: 4050 kN.m (2980 kip.ft)	$f_{ps}/f_{pu} = 0.79$ 3320 kN.m (2440 kip.ft)
	Nominal moment capacity (M_n)	South: 3550 kN.m (2620 kip.ft) North: 4050 kN.m (2980 kip.ft)	3320 kN.m (2440 kip.ft)

CONCLUSIONS

The 27 m (90 ft) continuous full-scale post-tensioned beam with unbonded tendons formed a full flexural failure mechanism under simulated uniform vertical forces. Prior to failure, the beam exhibited a large deformation capacity reaching midspan deflections of approximately $L/65$. Measured and inferred peak strand stress exceeded estimates obtained using current practice.

Failure of the beam occurred after a strand fractured somewhere along the beam length at an applied uniform load that exceeded the calculated nominal capacity by a factor of approximately 1.25 (in accordance with ACI 318-19 AASHTO LRFD Bridge Design Specifications, eighth edition). Test results suggest that for comparable beams, the use of limit analysis and current code provisions should provide safe estimates of the load-carrying capacity.

AUTHOR BIOS

Santiago Pujol, *FACI, is a Professor of Civil Engineering at the University of Canterbury, Christchurch, New Zealand. His is a member of ACI Committee 314, Simplified Design of Concrete Buildings; ACI Subcommittees 318-F, Foundations, and 318-W, Wind Provisions; and Joint ACI-ASCE Committees 441, Reinforced Concrete Columns, and 445, Shear and Torsion. His research interests include seismic vulnerability, structural testing and instrumentation, and repair and strengthening of structures.*

ACI member **Damon R. Fick** *is an Assistant Professor in the Civil Engineering Department at Montana State University, Bozeman, MT. He is Secretary of Joint ACI-ASCE Committee 352, Joints and Connections in Monolithic Concrete Structures, and a member of ACI Subcommittees 318-B, Anchorage and Reinforcement, and 318-J, Joints and Connections. His research interests include the behavior and design of reinforced concrete and bridge structures.*

ACI member **Luis B. Fargier-Gabaldón** *is the Massman-Beavers Associate Professor of Practice in Heavy Civil Engineering at the University of Notre Dame. He is member of ACI Subcommittee 318-F, Foundations, and Joint ACI-ASCE Committee 335, Composite and Hybrid Structures. His research interests include reinforced and prestressed concrete, soil-structure interaction, and bridge engineering.*

ACKNOWLEDGMENTS

R. Poston was instrumental in the conception and execution of the test and his help is much appreciated. Details of the test were conceived and directed by the late M. A. Sozen. Sozen probably knew well what the test was going to produce, but he held observation above almost everything else in engineering (except perhaps equilibrium, geometry, and virtual work that he sometimes said was nothing but equilibrium). His wisdom will be warmly remembered.

REFERENCES

AASHTO, 2018, *AASHTO LRFD Bridge Design Specifications*, eighth edition, American Association of State Highway and Transportation Officials, Washington, DC.

ACI Committee 318, 2019, "Building Code Requirements for Structural Concrete (ACI 318-19) and Commentary (ACI 318R-19)," American Concrete Institute, Farmington Hills, MI, 624 pp.

Aparicio, A. C.; Ramos, G.; and Casas, J. R., 2002, "Testing of Externally Prestressed Concrete Beams," *Engineering Structures*, V. 24, No. 1, pp. 73-84. doi: 10.1016/S0141-0296(01)00062-1

Aravinthan, T.; Mutsuyoshi, H.; Matupayont, S.; and Machida, A., 1996, "Moment Redistribution in Prestressed Concrete Continuous Beams with External Tendons," *Transactions of the Japan Concrete Institute*, V. 17, pp. 197-202.

Aravinthan, T.; Witchukreangkrai, E.; and Mutsuyoshi, H., 2005, "Flexural Behavior of Two-Span Continuous Prestressed Concrete Girders with Highly Eccentric External Tendons," *ACI Structural Journal*, V. 102, No. 3, May-June, pp. 402-411.

Burns, N. H.; Charney, F. A.; and Vines, W. R., 1978, "Tests of One-Way Post-Tensioned Slabs with Unbonded Tendons," *PCI Journal*, V. 23, No. 5, pp. 66-83. doi: 10.15554/pcij.09011978.66.83

Burns, N. H.; Helwig, T.; and Tsujimoto, T., 1991, "Effective Prestress Force in Continuous Post-Tensioned Beams with Un-Bonded Tendons," *ACI Structural Journal*, V. 88, No. 1, Jan.-Feb., pp. 84-90.

Burns, N. H., and Hemakom, R., 1977, "Test Scale Model of Post-Tensioned Flat Plate," *Journal of the Structural Division*, V. 103, No. 6, pp. 1237-1255. doi: 10.1061/JSDEAG.0004650

Campbell, T. I., and Chouinard, K. L., 1991, "Inñuence of Nonprestressed Reinforcement on the Strength of Unbonded Partially Concrete Members," *ACI Structural Journal*, V. 88, No. 5, Sept.-Oct., pp. 546-551.

Chakrabarti, P. R., 1995, "Ultimate Stress for Unbonded Post-Tensioning Tendons in Partially Prestressed Beams," *ACI Structural Journal*, V. 92, No. 6, Nov.-Dec., pp. 689-697.

Chen, R. J., 1971, "The Strength and Behavior of Post-Tensioned Prestressed Concrete Slabs with Unbonded Tendons," MSc thesis, University of Texas at Austin, Austin, TX.

Cooke, N.; Park, R.; and Yong, P., 1981, "Flexural Strength of Prestressed Concrete Members with Unbonded Tendons," *PCI Journal*, V. 26, No. 6, pp. 52-80. doi: 10.15554/pcij.11011981.52.81

Decheng, K., 2009, "Strengthening of RC Beams and Frames by External Prestressing," PhD thesis, National University of Singapore, Singapore.

Du, G., and Tao, X., 1985, "Ultimate Stress of Unbonded Tendons in Partially Prestressed Concrete Beams," *PCI Journal*, V. 30, No. 6, pp. 72-91. doi: 10.15554/pcij.11011985.72.91

Gebre-Michael, Z., 1970, "Behavior of Post-Tensioned Slabs with Unbonded Reinforcement," MSc thesis, University of Texas at Austin, Austin, TX.

Harajli, M. H., and Kanj, M. Y., 1992, "Service Load Behavior of Concrete Members Prestressed with Unbonded Tendons," *Journal of Structural Engineering*, ASCE, V. 118, No. 9, pp. 2569-2589. doi: 10.1061/(ASCE)0733-9445(1992)118:9(2569)

Harajli, M. H.; Mabsout, M. E.; and Al-Hajj, J. A., 2002, "Response of Externally Post-Tensioned Continuous Members," *ACI Structural Journal*, V. 99, No. 5, Sept.-Oct., pp. 671-680.

Hemakom, R., 1970, "Behavior of Post-Tensioned Prestressed Concrete Slabs with Unbonded Reinforcement," MSc thesis, University of Texas at Austin, Austin, TX.

Kosut, G.; Burns, N.; and Winter, C., 1985, "Test of Four-Panel Post-Tensioned Fat Plate," *Journal of Structural Engineering*, ASCE, V. 111, No. 9, pp. 1916-1929. doi: 10.1061/(ASCE)0733-9445(1985)111:9(1916)

Lou, T.; Lopes, S. M.; and Lopes, A. V., 2013, "Flexural Response of Continuous Concrete Beams Prestressed with External Tendons," *Journal of Bridge Engineering*, ASCE, V. 18, No. 6, pp. 525-537. doi: 10.1061/(ASCE)BE.1943-5592.0000392

Maguire, A. M.; Chang, M.; Collins, W.; and Sun, Y., 2017, "Stress Increase of Unbonded Tendons in Continuous Posttensioned Members," *Journal of Bridge Engineering*, ASCE, V. 22, No. 2. doi: 10.1061/(ASCE)BE.1943-5592.0000991

Maguire, M.; Collins, W. M.; Halbe, K. R.; and Roberts-Wollmann, C. L., 2015, "Multi-Span Members with Unbonded Tendons: Ultimate Strength Behavior," *ACI Structural Journal*, V. 113, No. 2, Mar.-Apr., pp. 195-204. doi: 10.14359/51688192

Mattock, A. H.; Yamazaki, J.; and Kattula, B., 1971, "Comparative Study of Prestressed Concrete Beams, with and without Bond," *ACI Journal Proceedings*, V. 68, No. 2, Feb., pp. 116-125.

Ng, C. K., "Tendon Stress and Flexural Strength of Externally Pre-Stressed Beams," 2003, *ACI Structural Journal*, V. 100, No. 5, Sept.-Oct., pp. 644-653.

Pannell, F. N., 1969, "The Ultimate Moment of Resistance of Unbonded Pre-Stressed Concrete Beams," *Magazine of Concrete Research*, V. 21, No. 66, pp. 43-54. doi: 10.1680/macr.1969.21.66.43

Tam, A., and Pannell, F. N., 1976, "The Ultimate Moment of Resistance of Unbonded Partially Prestressed Reinforced Concrete Beams," *Magazine of Concrete Research*, V. 28, No. 97, pp. 203-208. doi: 10.1680/macr.1976.28.97.203

Tan, K. H., and Ng, C. K., 1997, "Effects of Deviators and Tendon Conðguration on Behavior of Externally Prestressed Beams," *ACI Structural Journal*, V. 94, No. 1, Jan.-Feb., pp. 13-22.

Tan, K. H., and Tjandra, R. A., 2007, "Strengthening of RC Continuous Beams by External Prestressing," *Journal of Structural Engineering*, ASCE, V. 133, No. 2, pp. 195-204. doi: 10.1061/(ASCE)0733-9445(2007)133:2(195)10.1061/(ASCE)0733

Zhou, W., and Zheng, W., 2014, "Unbonded Tendons Stresses in Continuous Post-Tensioned Beams," *ACI Structural Journal*, V. 111, No. 3, May-June, pp. 525-536. doi: 10.14359/51686569